Cathodoluminescing properties of spark-processed silicon

1995 J. Phys.: Condens. Matter 7 9081

(http://iopscience.iop.org/0953-8984/7/47/024)

J. Phys.: Condens. Matter 7 (1995) 9081–9089. Printed in the UK

Cathodoluminescing properties of spark-processed silicon

M H Ludwig†, J Menniger‡ and R E Hummel†

† University of Florida, Department of Materials Science and Engineering, PO Box 116400, Gainesville, FL 32611-6400, USA

‡ Paul-Drude-Institut für Festkörperelektronik, Hausvogteiplatz 5-7, D-10117 Berlin, Germany

Received 2 March 1995, in final form 6 June 1995

Abstract. Spark-processed Si was characterized by temperature-dependent cathodoluminescence (CL) measurements. The CL spectra were recorded between 6 and 300 K. Two separated CL maxima were observed. The high-energy peak centred around 480 nm and the low-energy peak near 650 nm. Whereas the intensity of the red CL increased at lower temperatures, the intensity of the blue CL had a maximum near 230 K and then decreased continuously with decreasing temperatures. The integrated intensity for both CL bands remained essentially constant at temperatures below 270 K. This behaviour is interpreted in terms of a competitive radiative mechanism. Furthermore, the localized distribution of cathodoluminescing centres across the surface of a sample was studied by spectrally resolved CL micrographs. The results are discussed in comparison with the photoluminescing characteristics of spark-processed Si and in the light of the luminescing properties of porous Si.

1. Introduction

The observation of visible photoluminescence from electrochemically etched Si [1, 2], has attracted wide attention. Besides chemical etching procedures the method of spark processing (sp) has been shown to generate a similar Si structure that strongly photoluminesces at room temperature [3, 4]. These results were principally confirmed by other authors [5, 6]. The photoluminescence (PL) spectra of sp-Si consist of a violet/blue emission band at 410 nm or a green emission centred at around 515 nm, depending on the conditions during spark processing. The PL intensities are comparable to those of the most efficient electrochemically etched (red luminescing) porous silicon specimens [4, 7]. Spark processing is a dry technique and applicable in different gaseous environments. The involvement of OH groups, hydrogen or fluorine can therefore be excluded as major contributors for the origin(s) of the PL of sp-Si [8, 9]. Furthermore, the PL of sp-Si also remains stable with respect to peak intensity and peak wavelength after etching in buffered HF up to 30 min which should substantially diminish the SiO_x layers present. These results indicate, that radiative recombinations via defect structures in SiO_x, as brought forward by others [10, 11], may not be considered as the principal origin for the PL of sp-Si. Moreover, photoluminescence is also observed when spark processing is applied to different indirect- and direct-bandgap semiconductors, causing PL peak wavelengths which are strongly blueshifted compared to the bandgap energies of the unprocessed samples. It was therefore proposed, that the luminescence mechanism is related to the presence of nanocrystalline structures as found by transmission electron microscopy or Raman measurements [12, 13].

The present study discusses the luminescing properties of sp-Si when exposed to a high-energy electron beam. The resulting cathodoluminescence (CL) spectra may

0953-8984/95/479081+09$19.50

provide additional information concerning the origin(s) of luminescence in these materials. Specifically, the correlation to silicon–oxygen related luminescence is considered, since there are several CL bands in amorphous SiO_2 which lie in the visible spectrum [14–16]. These investigations are particularly done in the light of recent findings that the generally orange–red-peaking CL for nanocrystalline, porous Si is superimposed by bright spots which emitted white, green or blue CL [17]. Thus, CL might prove a useful probe for characterizing the localized structure or non-uniformity of luminescence.

2. The experiment

Spark processing of silicon has been accomplished by utilizing a unidirectional high voltage (15 kV) discharge between a tungsten tip (anode) and a Si wafer (cathode). Each spark consisted of a single pulse (having a duration of about 0.02 μs) which was repeated every 60 μs. The tungsten tip was positioned 1 mm above the Si surface. Two procedures were utilized for spark processing. One type of sample was spark-processed while blowing dry, compressed air on the Si surface. Another type of sp-Si was prepared in stagnant air. All experiments were performed at room temperature. The spark-processing time was two hours. The Si samples were cut from the same wafer, which was p-type doped by boron ($\sim 6 \times 10^{18}$ cm^{-3}).

The steady-state CL characterizations were performed in a scanning electron microscope equipped with an Oxford Mono-CL and a He cooling stage system. The spectra were measured in the wavelength range from 250 to 800 nm at temperatures between 6 and 310 K. The electron beam was accelerated by applying 10 keV and the beam current was held at 28 nA. For each temperature the same position at the surface of a given spark-processed sample was scanned, investigating thereby an area of 163×225 μm^2. The surface topography was observed by secondary-electron (SE) micrographs.

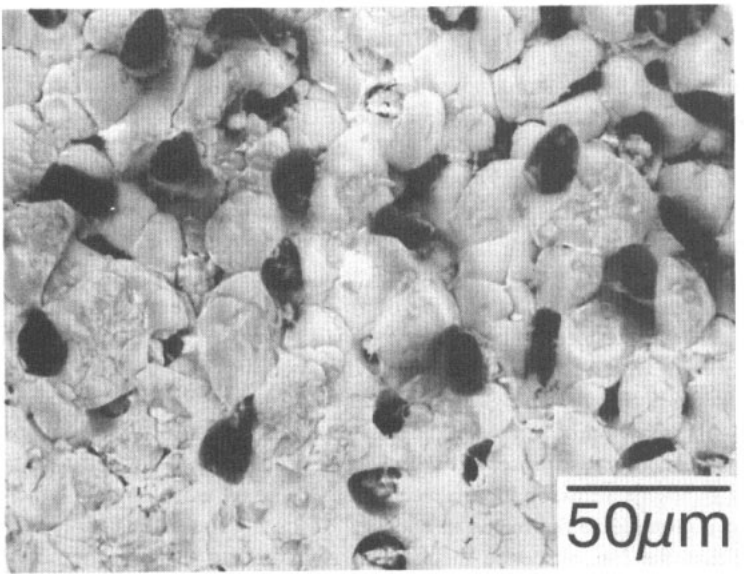

Figure 1. A SE image of the surface of spark-processed Si. The holes have an average diameter of 15 μm and are caused by flash evaporation, induced by the spark impact.

3. Results and discussion

Figure 1 depicts an SE image which is typical for a spark-processed Si surface. The area is characterized by black spots, that is, by holes having a typical diameter of about 15 μm. These holes originate from spark impacts which are assumed to flash-evaporate a certain amount of Si. Since the spark process consists of a pulsed discharge, the Si vapour is allowed to redeposit randomly during off times, thus creating a crater-like structure. A study of the cross-sectional view at the centre of the spark-processed layer revealed that the holes extend to channels having a length of at least 250 μm within an overall sp-layer thickness of about 400 μm. The noticed charging effects during imaging (white areas in the lower left corner of figure 1) indicate a considerably increased electrical resistance. This observation is in agreement with our previous findings that spark-processing in air generates an amorphous SiO_x matrix with imbedded Si nanocrystallites [4, 18].

Figure 2 shows a comparison between SE and spectrally resolved CL micrographs (480 and 670 nm) taken from the same area of the sample. Each measurement for figure 2 was performed at 6 K. It was observed that the hole area, which is the black region in the SEM picture, emitted the highest CL intensity, three to five times more than the surroundings. We noticed a comparably enhanced CL also in a cross-sectional view of spark holes, which indicates that the higher output does not result from light guiding effects. Additionally, the CL micrographs in figures 2(b) and 2(c) show some fuzzy and some sharp, point-like structures. The latter were very bright, but could not be analysed further, because they degraded rapidly under the electron beam. The white areas in the SE image (figure 2(a)) were again caused by charging effects. It should be particularly emphasized that the hole itself is not subject to charging.

The blue CL is characterized by a considerably slower decay than the red CL emitted from the same position. This is concluded from a halo-like afterglow seen in figure 2(b). The blue CL emitted by the hole appears to be extended somewhat to the right-hand side of the image. This effect is caused by a faster scanning of the image by the electron beam compared to the decay time of the cathodoluminescence as detected by the photomultiplier. Since the CL is always observed for the entire image and then assigned to the current position of the scanning electron beam to create the CL micrograph, the signal of a very slowly decaying CL will still be recorded when the exciting beam has already moved to the next location, thus generating an afterglow. By knowing that each of the 512 pixels of a horizontal line was scanned for 0.8 ms, the blue decay time can be estimated to be in the order of about 50 ms. The decay time for the red CL is estimated to be faster than that of the blue CL by at least one order of magnitude since there is no afterglow effect detectable for the red cathodoluminescence (figure 2(c)). A similar time-delayed blue photoluminescence was reported for strongly oxidized porous Si by Kux *et al* [19]. They observed a time constant of the order of 1 s when utilizing a high-energy ($\geqslant$ 4.3 eV) optical excitation source. However, spark-processed Si, measured under comparable conditions as described by Kux [19], did not display a corresponding slow component of the blue photoluminescence.

For recording the CL as a function of temperature a representative region was chosen and kept fixed during the entire cooling cycle. The measured spectra are summarized in figure 3 in a three-dimensional representation. Two CL bands were found. First, a blue, high-energy band centred at 480 nm provides the dominant luminescence at room temperature. Second, a red band peaks near 640 nm at room temperature. It should be particularly emphasized that identical spectra were obtained for both types of samples (prepared by spark-processing in stagnant air and with blowing air). This is in contrast to photoluminescence experiments

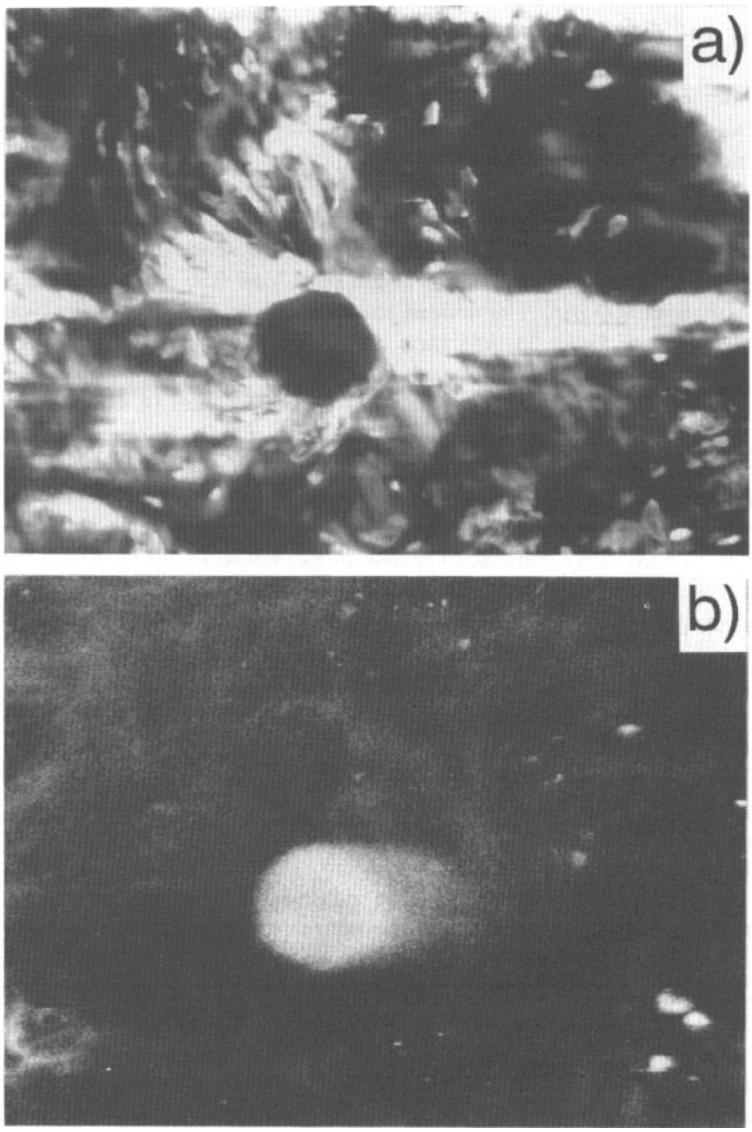

Figure 2. Comparison of the same hole structure for sp-Si, recorded at 6 K: (a) a SE image; the hole appears black (the white areas result from charging effects); (b) a CL micrograph utilizing a detection wavelength of 480 nm; (c) a CL micrograph with a detection wavelength of 670 nm.

for which we found different PL peak wavelengths (410 nm or 515 nm, when excited at 325 nm HeCd) [4]. Thus, the PL and the CL spectra are not identical in their distribution of excited wavelengths.

Figure 3 further displays distinctly different temperature dependences for the red and the blue CL intensities. These results can be seen in more detail in figure 4, where the integrated CL intensities for both bands are displayed as a function of temperature. Toward lower temperatures the intensity of the blue CL first increases slightly, having a maximum around 220 K and then decreases continuously. The red CL intensity instead increases

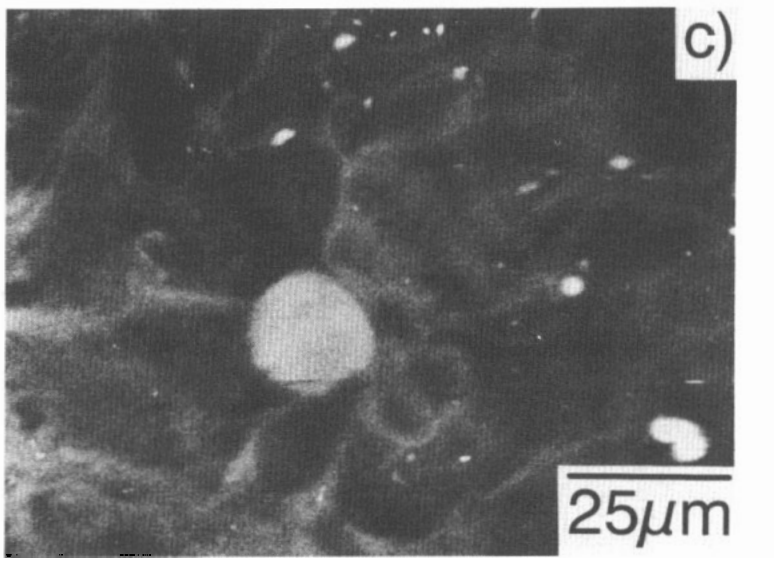

Figure 2. (Continued)

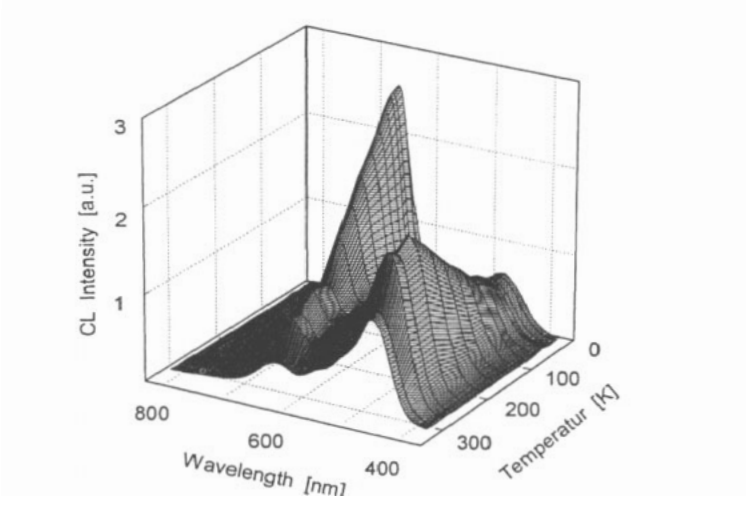

Figure 3. A 3D display of a series of cathodoluminescence spectra taken on sp-Si recorded in the temperature range from 5 to 310 K.

steadily by cooling to 5 K. The temperature dependence of the integrated CL intensity $I(T)$ for the red band can be well described by the empirical expression [20]

$$I(T) = I_0/[1 + c\exp(T/T_0)]. \tag{1}$$

Equation (1) describes the temperature dependence of luminescence in disordered solids in terms of a characteristic temperature T_0, which is a measure of the system disorder and related to the tail width of the density of localized states in the gap region. The constant c in equation (1) is temperature independent. The data points for the red CL have been fitted by using equation (1) and shown by the solid line in figure 4. For the characteristic

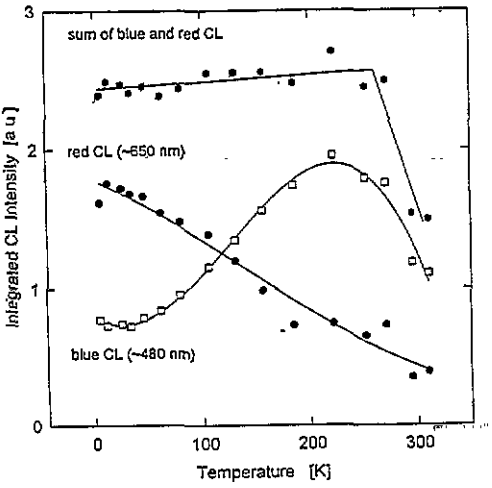

Figure 4. The temperature dependence of the integrated cathodoluminescence intensities of sp-Si for the red band (curve fitted according to equation (1)), the blue band (curve to guide the eye) and the sum of the overall measured CL intensity (curve to guide the eye).

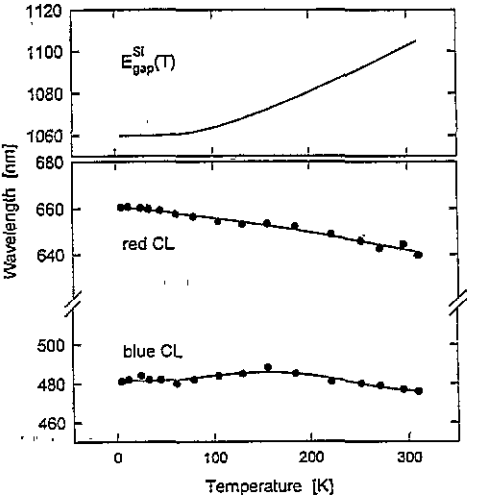

Figure 5. The temperature dependence of CL peak wavelengths of sp-Si, and that of the bulk silicon bandgap, separated in the upper section.

temperature T_0 a value of ~ 97 K (i.e. $kT_0 = 8$ meV) was found, which is indicative of the existence of disorder [21]. The temperature behaviour of the blue CL intensity cannot be described satisfactorily by the same expression. The fitted line for the blue CL in figure 4 is only a guide for the eye.

Also included in figure 4 are the data for the summarized integrated CL intensities of the blue and red cathodoluminescence of sp-Si. The main feature is the nearly constant value for temperatures below 270 K. The apparent conservation in the total integrated intensity suggests a competitive or compensating mechanism for the radiative recombination of the two bands. The competitive model implies a direct conversion of excited electrons from the blue to the red channel when lowering the temperature. In other words the reduction of the blue CL intensity is compensated by the increase in red CL intensity and vice versa. In order to explain the competitive radiative model, it is necessary to assume a recombination rate for the blue CL which is smaller compared to that of the red channel at low temperatures. This assumption is in contrast to the results of decay time measurements for the PL of sp-Si [22] where the decay time constants were found to be in the ns range for the entire spectrum (i.e., the violet/blue PL as well as the red tail-part of the PL spectrum). On the other hand, as stated above in the discussion of figure 2, the decay time of the blue CL (~ 480 nm) was estimated to be about 50 ms at 6 K and that of the red CL much shorter. Therefore, the competitive mechanism is reasonable for the description of the CL temperature dependence. Furthermore, the comparison between PL and CL decay behaviour of sp-Si reveals decisive differences for both types of excitation.

Figure 5 depicts the wavelength shifts of the blue and red CL bands, detected in the maximum, versus temperature. The blue CL peak remains nearly constant over the entire temperature range, having only a slightly larger value around 150 K, followed by a minor tendency to decrease for higher temperatures. The temperature behaviour of the red band

is much more pronounced. From 6 to 310 K a continuous shift to lower wavelengths was observed. In well ordered semiconductors, the energies emitted by a radiative recombination of free and bound excitons follow the bandgap. For comparison the wavelength shift for the Si bandgap over the temperature range in question is shown in the upper part of figure 5. It is evident that the temperature dependencies of both CL peaks do not follow that of the bandgap of bulk material. A similarly opposite behaviour is known for transitions which occur in amorphous semiconductors with strongly localized wavefunctions. For example, the PL peak position in silicon oxynitride films was found to downshift in wavelength for temperatures above 100 K [23].

Frequent features of a number of previous CL studies on SiO_2 layers are bands at 650 nm, 460–560 nm, and 280–290 nm [14, 16, 24, 25]. In discussing the dissimilarities between the CL and PL spectra of sp-Si one should consider the different excitation conditions. The 10 kV electron beam provides sufficient energy to excite electrons into absorption bands around 5.4 and 4.8 eV which are known to occur in amorphous silicon oxide. Both absorption bands are associated with luminescence bands, the one at higher energy with emission bands in the UV (280–290 nm) and the blue/green (460–560 nm) spectral range, the one at 4.8 eV is related to a red/orange emission (620–650 nm).

An interesting model for the blue/green luminescence was proposed by Mitchell *et al* [14] by assigning it to a trivalent Si centre, located principally near the oxygen-deficient Si/SiO_2 interface. As shown above, the CL intensities from sp-Si are obviously enhanced at the hole structures. The holes themselves are thought to be generated in a flash evaporation process caused by a spark discharge, which is an event with a timescale of about 20 ns. This period is assumed to be too short for a sufficient intermixing between the Si vapour phase and ambient air to create stoichiometric silicon oxide, thus resulting in a Si-rich, redeposited $Si–SiO_x$ layer at the inner walls of the 'worm holes'. In other words, the specific conditions of an oxygen-deficient Si/SiO_2 interface are repeated, but in a larger geometric scale per unit area compared to a 'virgin' Si wafer surface. The presence of SiO_x alone is definitely not enough to initiate blue cathodoluminescence as shown very clearly in figures 2(b) and 2(c). Almost no emissions were detected from the surroundings of the hole, even though the presence of a high content of insulating SiO_x is impressively demonstrated by the charging effects in the SE image (figure 2(a)).

The 650 nm emission is commonly addressed to nonbridging oxygen centres (NBOC) having an absorption band at 4.8 eV [16, 25]. These centres are often found in radiation-damaged or electron-bombarded silica. As the spark discharge involves highly accelerated electrons and ions, the generation of similar defects is likely to occur in the proximity of spark-generated holes in silicon. NBOCs are therefore suggested to be responsible for the red CL band of sp-Si.

CL measurements provide a sensitive tool for investigating (*inter alia*) layers on Si, where PL is normally not efficient enough to produce a passable signal-to-noise ratio. Naturally, the PL efficiency depends on the absorption coefficient which is effective for the excitation wavelength used. The 325 nm (3.8 eV) laser line we utilized in our PL experiments is energetically not sufficient to efficiently trigger the above-discussed absorption bands. Consequently, we should not observe the associated luminescence bands. However, an intense PL response was found—although, neither the blue/green nor the red CL bands are present in the PL spectra of sp-Si. Moreover, the PL peak wavelength shift in the spectral range between 410 and 560 nm depending on the preparation conditions during spark-processing [4, 7], whereas the CL spectra of the same specimen stay essentially the same. These results strongly indicate that different mechanisms are contributing to the luminescing properties of CL and PL spectra of sp-Si.

This conclusion is supported by taking the penetration depths into account which are characteristic for the 325 nm laser line and for the 10 kV electron beam. Spark-processed silicon is considered to consist of Si nanocrystallites imbedded in an amorphous SiO_2 and/or SiO_x matrix [18] (depending on the processing parameters). Amorphous SiO_2 is almost transparent for the exciting photons, possibly leaving Si clusters as the main absorption centres. For $SiO_{1.5}$ having an absorption coefficient of approximately 10^3 cm^{-1} at 325 nm [26] the characteristic penetration depth equals about 10 μm. The depth distribution of the primary electrons in the CL experiments can be calculated by using Kanaya's range–energy relation [27]. The maximum penetration depth for electrons accelerated by 10 kV towards SiO_x is about 8 μm and the centre of the distribution lies at a depth of 2.5–3 μm. The diffusion lengths of electrons in silicon dioxide are too short (of the order of 3–5 nm) to broaden the distribution. It is therefore reasonable to assume that the UV laser light is capable of exciting deeper-lying structures which might be responsible for the intense violet/blue PL at 410 nm or the green PL around 515 nm, whereas the CL spectra are more surface related in comparison.

4. Conclusions

CL spectra taken on sp-Si display two emission bands, centred at 480 nm and around 650 nm. The CL spectra differ in peak wavelengths and distribution from PL spectra of the same material. Varied preparation conditions during spark-processing cause different wavelength maxima in the PL, whereas the CL spectra stay essentially alike.

The CL intensity is not uniformly distributed across a given sp-Si surface. Specifically, the most intense CL was found at the holes, which were created by spark-processing. At low temperatures the decay time for the blue CL (emitted by the hole structures) increases to an estimated value of about 50 ms at 6 K. The decay time for the red band was found to be shorter by at least one order of magnitude.

During cooling, competitive behaviour between the blue and the red cathodoluminescing channels was observed. The blue CL lost about the same amount of intensity as the red CL gained. This is interpreted in terms of a direct conversion of excited electrons from high-energy (blue) to lower-energy (red) recombination channels. Both CL bands are characterized by strong-disorder effects.

The present study therefore suggests that CL and PL derive their light emissions from different mechanisms and probably from dissimilar morphological configurations of sp-Si. Whereas the electron beam is expected to excite the topmost layer, the UV laser beam is capable of penetrating SiO_x, thus exciting deeper-lying structures, which are covered by silicon oxide.

Acknowledgments

One of the authors (MHL) gratefully acknowledges the financial support by a Habilitationsstipendium provided by the Deutsche Forschungsgemeinschaft. We are indebted to ARPA for financial assistance and to Wacker Chemitronic for supplying the wafer material.

References

[1] Canham L T 1990 *Appl. Phys. Lett.* **57** 1046
[2] Lehmann V and Gösele U 1991 *Appl. Phys. Lett.* **58** 856
[3] Hummel R E and Chang S-S 1992 *Appl. Phys. Lett.* **61** 1965

[4] Hummel R E, Ludwig M H and Chang S-S 1995 *Solid State Commun.* **93** 237
[5] Rüter D and Bauhofer W 1993 *J. Lumin.* **57** 19
[6] Steigmeier E F, Auderset H, Delley B and Morf R 1993 *J. Lumin.* **57** 9
[7] Hummel R E, Ludwig M H, Chang S-S and LaTorre G 1995 *Thin Solid Films* **255** 219
[8] Hummel R E, Ludwig M H, Hack J and Chang S-S 1995 *Solid State Commun.* at press
[9] Hummel R E, Ludwig M H and Chang S-S 1995 *Mater. Res. Soc. Symp. Proc.* **358** 151
[10] Prokes S 1993 *Appl. Phys. Lett.* **62** 3244
[11] Nozaki S, Sato S, Ono H and Morisaki H 1994 *Mater. Res. Soc. Symp. Proc.* **351** 399
[12] Ludwig M H, Hummel R E and Chang S-S 1994 *J. Vac. Sci. Technol.* B **12** 3023
[13] Ludwig M H, Hummel R E and Stora M 1995 *Thin Solid Films* **255** 103
[14] Mitchell J P and Denure D G 1973 *Solid-State Electron* **16** 825
[15] Koyama 1980 *J. Appl. Phys.* **51** 2228
[16] Skuja L N and Entzian W 1986 *Phys. Status Solidi* a **96** 191
[17] Chen X, Uttamchandani D, Trager-Cowan C and O'Donnell K P 1993 *Semicond. Sci. Technol.* **8** 92
[18] Hummel R E, Morrone A, Ludwig M H and Chang S-S 1993 *Appl. Phys. Lett.* **63** 2711
[19] Kux A, Kovalev D and Koch F 1995 *Thin Solid Films* **143** 305
[20] Collins R W, Paesler M A and Paul W 1980 *Solid State Commun.* **34** 833
[21] Bayliss S C, Anstee P, Hutt D A, Zhang Q, Danson N, Bates J and Waddilove A 1994 *J. Appl. Phys.* **76** 5171
[22] Hummel R E, Fauchet P M, Ludwig M H, Vandyshev Ju V, Chang S-S and Tsybeskov L 1995 *Solid State Commun.* **95** 553
[23] Fischer K, Muschik T, Schwarz R, Kovalev D and Koch F 1995 *Mater. Res. Soc. Symp. Proc.* **358** 851
[24] Pio F, Guzzi M, Spinolo G and Martini M 1990 *Phys. Status Solidi* b **159** 577
[25] Cullis A G, Canham L T, Williams G M, Smith P W and Dosser O D 1994 *J. Appl. Phys.* **75** 493
[26] Philipp H R 1971 *J. Phys. Chem. Solids* **32** 1935
[27] Kanaya K and Okayama S 1972 *J. Phys. D: Appl. Phys.* **5** 43